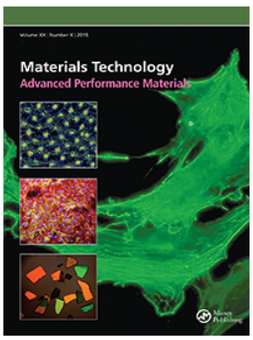

Taylor & Francis
Taylor & Francis Group

Materials Technology
Advanced Performance Materials

ISSN: 1066-7857 (Print) 1753-5557 (Online) Journal homepage: https://www.tandfonline.com/loi/ymte20

Preparation of active antimicrobial and antifungal alginate-montmorillonite/lemon essential oil nanocomposite films

Naima Hammoudi, Hocine Ziani Cherif, Fethi Borsali, Kamal Benmansour & Asma Meghezzi

To cite this article: Naima Hammoudi, Hocine Ziani Cherif, Fethi Borsali, Kamal Benmansour & Asma Meghezzi (2019): Preparation of active antimicrobial and antifungal alginate-montmorillonite/lemon essential oil nanocomposite films, Materials Technology, DOI: 10.1080/10667857.2019.1685292

To link to this article: https://doi.org/10.1080/10667857.2019.1685292

Published online: 11 Dec 2019.

MATERIALS TECHNOLOGY
https://doi.org/10.1080/10667857.2019.1685292

Preparation of active antimicrobial and antifungal alginate-montmorillonite/lemon essential oil nanocomposite films

Naima Hammoudi[a], Hocine Ziani Cherif[a], Fethi Borsali[b], Kamal Benmansour[a] and Asma Meghezzi[c]

[a]Macromolecular Research Laboratory, Tlemcen University, Tlemcen, Algeria; [b]Laboratoire Systèmes Dynamiques et Applications, Tlemcen University, Tlemcen, Algeria; [c]Laboratory of microbiology and bioprocesses - Nutrition and food science - Food Biotechnology Division, C.R.Bt Biotechnology Research Center, Constantine, Algeria

ABSTRACT

The inclusion of antimicrobial and antifungal agents such as essential oils directly into a food packaging material is a form of active packaging elaboration. In this work, alginate-based films activated with lemon essential oil (LEO) at increasing concentration levels [0.5%, 1% and 1.5% (v/v)] were prepared, and their antibacterial and antifungal activities were investigated. The microstructure characterisation of alginate-montmorillonite/LEO (alg-MMT/LEO) nanocomposites was performed using X-ray diffraction (XRD) and Fourier transform infrared spectroscopy (FTIR) and the surface morphology of the films was examined using light microscopy. The XRD and FTIR results confirmed MMT exfoliation and revealed the presence of strong interaction between alginate and MMT in the presence of LEO. Thermogravimetric analysis (TGA) indicated that LEO-containing films exhibited a higher degradation temperature in comparison with pure alginate films. Powerful antimicrobial and antifungal properties of the films were also highlighted at 1.5% LEO concentration, suggesting that the formulated nanocomposites might be considered as promising active packaging materials.

ARTICLE HISTORY
Received 30 April 2019
Accepted 22 October 2019

KEYWORDS
Bionanocomposite; alginate; montmorillonite; lemon essential oil; food packaging

Introduction

The vast majority of commonly known 'plastics' are organic synthetic processed materials using petroleum both as feedstock and as energy during manufacture. The environmental concerns of the oil-based economy are being widely voiced as executive governmental policies and large impact companies hardly attempt to reduce their carbon footprints. On another related but stressing issue, that of worldwide waste management, studies on the ecological footprint of humanity have suggested that sustainability of human pressures on the world's ecological resources shifted from 70% of global regenerative capacity in the 1960s to more than 120% today. As a response deriving from a normal physical law of action and reaction, the quest for a solution to this dramatic situation has been launched just few decades ago. This holy and hopefully not Sisyphean search for alternatives to traditional petroleum-based plastics is progressing at a pace that at the outcome, not just the source, but also the downstream consequences will be bypassed. In this endeavour, impressive efforts were focused on biopolymers. Their prominent position within the realm of natural substances propelled them obviously to the centre stage over the last two decades, since they provide a viable alternative to the environmentally harmful waste disposal of plastic foods packaging materials. Another interesting feature of this naturally occurring materials is that biopolymer films are considered as excellent vehicles for the inclusion of a wide variety of additives, such as antioxidants, antifungal agents, antimicrobials and other nutrients [1,2]. Consequently, these biodegradable materials might play a positive role in improving food quality in terms of packaging and storage commodities by imparting shelf life extension and minimisation of microbial growth in the product. Alginates, a naturally occurring polysaccharides found in seaweed in the form of calcium, magnesium and sodium salts, are made of two urinate sugars (mannuronate and guluronate) as building blocks, which are obtained in the form of sodium salts of mannuronic and guluronic acid, respectively, during alginates extraction and neutralisation process (Figure 1). The ratio and distribution of these blocks will determine the alginate properties while the composition varies according to seaweed species and structure.

In the course of these studies, some relevant aspects of sodium alginate related to its rheological and chemical properties have attracted our attention. These include the viscosity increase through solution thickening effect and a tight binding to calcium, eventually leading to versatile and interesting gel- or film-forming applications. It also acts as stabiliser and emulsifier. However, alginate's poor mechanical and gas barrier properties, as well as weak water resistance hamper its proper use particularly in the presence of water or humidity. More recently, remarkable improvements in the functional properties of these films have been made by reinforcement of the polymer

CONTACT Kamal Benmansour kamal.benmansour@mail.univ-tlemcen.dz Macromolecular Research Laboratory, Tlemcen University, Tlemcen, Algeria

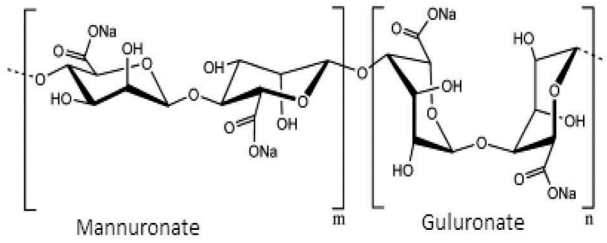

Figure 1. The molecular structure of sodium alginate.

matrix with layered silicates [3–7]. Outstanding and successfully crowned efforts have been reported in the literature whose main purpose was aimed at improving a whole range of alginate film's fundamental characteristics, such as mechanical and functional properties, thermal stability, barrier properties, and water solubility through incorporation of a nanoclay into alginate. Particularly, montmorillonite (MMT) which is a hydrated alumina-silicate-layered clay consisting of an edge-shared octahedral sheet of aluminium hydroxide sandwiched between two silica tetrahedral layers was the most extensively studied. The imbalance of the surface negative charges is largely compensated by exchangeable cations (typically Na^+ and Ca^{2+}). In the next task as a technological step forward, films exhibiting antimicrobial properties could be produced upon addition of antimicrobial agents, including either the commonly known inorganic compounds such as TiO_2, Ag, ZnO, and MgO nanoparticles, or natural organic additives [8–12]. Indeed, an abundant literature focusing on the antimicrobial activity of some selected metals such as titanium, silver and copper derivatives, and its fine-tuning through blending or nanostructuring, eventually leading to its spectacular enhancement, is recently flourishing. Naturally, the potential of these advanced properties paved the way for their promising use primarily in solid-state hybrid materials, and more particularly in biomedical devices such as metallic implants [13–18].

However, one major issue of concern in using synthetic antimicrobials as film additives stems from their toxicity hazards as they may inauspiciously diffuse into the polymer matrix. Besides their historical central position in perfumery, essential oils (EOs) have been widely used for their numerous properties in phytotherapy, pharmacy and cosmetics. Yet, their seemingly limitless virtues propelled them once again at the front scene of natural products-based commodities. Carbogenic antimicrobial agents deriving from natural sources – such as essential oils (EOs) – were largely coveted for their natural antimicrobial activities [19]. Indeed, essential oils possessing antimicrobial activity play a key role in the mechanism of the reduction of virulence and pathogenicity of bacteria. Their antimicrobial activity effectiveness as film's additives is determined in part by the rate of releasing process. In case of too slow release, the microbial growth would not be sufficiently inhibited, and oppositely, a too fast release would beget a non-sustained inhibition [20]. The rate of release depends also on other various parameters including the type of polymer, film preparation method, nature of interactions between polymeric and antimicrobial agents [21], and environmental conditions [22,23]. Montmorillonite may potentially serve to control the release of antimicrobial agents from film materials. Although several reports on alginate/clay nanocomposites have appeared in the literature, to our knowledge, few studies are available on the combined effect of nanoclay and antimicrobial compounds such as EOs. On hypothetic ground, we assumed that the combination of a nanoclay and an antimicrobial compound entrapped within alginate films should lead to a material bestowed with interesting functionalities without altering the bulk properties nor the structural integrity of the composite. Barrier properties would mainly be imparted by the nanocomposite matrix while antimicrobial activity provided by the loaded and conveniently selected essential oil. In addition, such nanocomposite films made strictly of natural biopolymers should be considered as environmentally friendly with all the downstream benefits one may expect from biopolymer and nanocomposite packaging materials [1]. Among the plethora of essential oils endowed with antibacterial activity against *E.coli* and *S. aureus*, lemon essential oil (*Citrus limon* L.), containing limonene, β-pinene, γ-terpinene and citral (neral and geranial) as main components showed interesting antimicrobial features [24–26]. In the present study, the combined effects of MMT and lemon essential oil (LEO) on the physicochemical, antimicrobial and antifungal properties of alginate composite films have been investigated.

Materials and methods

Materials

Sodium alginate (medium viscosity), montmorillonite (MMT) and glycerol were obtained from Sigma-Aldrich Co. Lemon (*Citrus limon* L.) essential oil was purchased from Aldrich chemical Co and stored in a sealed dark container at 6°C. Tween 80 was purchased from Merck, Germany.

Biological material

Six reference microbial and fungal strains were used for the antibiogram test. The strains were *Staphylococcus aureus* (ATTC 25,923); *Salmonella enteritidis* (ATCC 13,076); *Escherichia coli* (ATCC 25,922) and *Bacillus cereus* (ATCC 6633); *Aspergillus baraziliensens* (ATCC 16,404) and the yeast *Candida albicans* (ATCC 10,230). All the stock cultures were generously provided by The Laboratory of microbiology and bioprocesses- C.R.B.T

Biotechnology Research Centre of Constantine -Algeria. The strains were transferred in brain heart infusion broth and grown in a shaker incubator to 37°C. The micro-organism suspensions were diluted with sterile peptone water. The bacterial population estimated at a wavelength λ = 620 nm reached a value of 0.4 which corresponded to a concentration of 10^6 UFC/ml.

Preparation of nanocomposite film

An aqueous solution of sodium alginate was prepared by dissolving 10 g of powdery sodium alginate in 1000 ml of distilled water (at 70°C) using a magnetic stirrer at 1200 rpm for 45 min to make a 1% w/v solution. Separately, a specific amount of MMT [(3% w/w)] based on solid sodium alginate contents] was dispersed in 50 mL of distilled water and stirred vigorously for 24 h at room temperature. The alginate solution was then slowly added to the preformed clay suspension and the resulting mixture was stirred for 4 h. A mixture of lemon essential oil and Tween 80 (0.25 g/g of essential oil) was added to the film-forming solution at different concentrations (0.5%, 1.0%, and 1.5% w/v on the basis of neat film solution). The final solution was homogenised at 1000 rpm for 5 min (*Ultra-Turrax homogeniser*), and the resulting mixture was degassed under vacuum for 30 min in order to remove all bubbles. Finally, the film-forming solution was cast onto Petri dishes (9 cm in diameter) and dried for 72 h at ambient conditions. The dried films were removed from the Petri dishes and preconditioned in desiccators containing saturated magnesium nitrate solution at 25°C.

Experimental techniques and characterisation

X-ray diffraction analysis

X-ray diffraction performed with a MiniFlex600 X-ray diffractometer was used for the measurement of the interredicular distance and determination of exfoliation rate, under the following conditions: F.F tube 40 kV and 15 mA. The films were exposed to Cu radiation at a wavelength of 1.54 nm. Alginate/MMT – LEO films were scanned over a 2θ diffraction angle interval = 2–10° and 2–40° with scan speed of 4°/min a steep interval of 0.01°.

Morphological study

The morphological study of the synthesised materials was carried out using light microscopy. The images were acquired with an Olympus SC40 Camera.

Fourier transformation infrared (FTIR) spectra

The Fourier transform infrared spectra of the nano-composite films were recorded with an Agilent Cary 640 FTIR spectrophotometer over the range 400–4000 cm^{-1} using a transmission method.

Thermal properties

TGA-DTA analysis of films was performed using a Linseis TGA PT1600 differential thermal analyser. Samples of 10–15 mg were heated to 800°C at a rate of 10°C/min under nitrogen atmosphere. The weight loss was measured as a function of temperature.

Measurement of film thickness

The film thickness was measured using an electronic outside micrometre having a sensitivity of 0.001 mm. Ten measurements were taken for each sample at different points.

Opacity

Opacity values of the films were determined using an Analytik jena, Specord 200 plus UV/VIS spectrophotometer. The films were cut in rectangular pieces and placed in the sample compartment of the spectrophotometer. An empty compartment was used as reference in the measurements. The absorbance spectra of the films were recorded over the range 200 to 800 nm, and opacity values of the films were calculated using the following equation:

$$\textbf{Opacity} = \textbf{Abs600}/\textbf{X}$$

where Abs 600 is the absorbance value at 600 nm and X, the film thickness (mm).

Microbiological analysis

Antibiogram test

The antibacterial effect of film-forming solution was studied using the agar diffusion test. The test was performed by applying 0,1 ml inoculums of *S. aureus, salmonella, E. coli, Bacillus Aspergillus*, and the yeast *Candida*, respectively, each containing approximately 10^4–10^5 CFU/ml, directly to the surface of a specific culture media poured in a Petri dish. Then, film-forming solution (8 µl) was cast onto discs (6 mm in diameter each) that were previously cut from Whatman filter paper n°3 and sterilised in hot air oven. The discs were placed in the Petri dish and incubated at 37°C for antibacterial test or 25°C for antifungal test during 24 h. All tests were done in triplicate.

Antimicrobial effectiveness of films

Twenty grams of TSA-NaCl were poured into Petri dishes (9 cm diameter). After solidification of the medium, 100 µl aliquots of the appropriately diluted bacterial suspension were inoculated on the surface of TSA-3% NaCl. Then, different films and the control (containing or not antimicrobial substances) having the same diameter as the Petri dishes, were placed on the inoculated surface. Inoculated and uncoated TSA-NaCl was used as control. The plates were stored at 10°C for 12 days. Microbial counts on TSA-3% NaCl plates were

examined immediately after inoculation and then regularly during the storage period. For this purpose, the agar was aseptically removed from Petri dishes and placed in sterile glass containers. One hundred milliliters of peptone water were added to each container and homogenised for 3 min, giving an homogeneous system. Cascade dilutions were made and then poured onto TSA. Plates were incubated at 37°C for 48 h before colonies were counted.

Statistical analyses

Statistical analysis was carried out with ANOVA IBM SPSS program (IBM SPSS statistic 21.Ink). Data were given as mean ± standard deviation for the treatment and Duncan's multiple range test determined the significant at $p < 0.05$ level.

Results and discussion

The elaboration of antimicrobial and antifungal nanocomposite plastic films that may be used in packaging commodities underscores the importance of a functionality-driven rational design using three components material. Alginate, which served as the core compound delivering the polymeric matrix, was modified with MMT nanoclay to improve mechanical, thermal and barrier properties of alginate films. Then, a homogeneous solution of lemon essential oil solubilised in the non-ionic hydrophilic emulsifier *Tween 80*® was added to alginate/MMT mixture. *Tween 80*® ensured a uniform and stable distribution of EO inside the polymeric matrix by virtue of its chemical nature and compatibility with alginate. The composite material was characterised by means of X-ray diffraction, FT-IR, SEM, TGA and DSC techniques. Microbiological assays were performed against *S. aureus, salmonella, E. coli, Bacillus, Aspergillus*, and the yeast *Candida*. The results of our investigations are disclosed in this paper.

XRD analysis

XRD images of MMT, pure sodium alginate, alg/MMT and alg/MMT-1.5% LEO nanocomposite films are shown in Figure 2. It appears (see expanded view in Figure 2) from pure clay's diffractogram that the diffraction peak of MMT's [001] plane is centred at $2\theta = 7.34°$ ($d = 12.03$Å). It is well established that intercalation of the polymer chains within the clay substructure usually increases the interlayer spacing, leading to a shift of the diffraction peak towards lower angle values. As far as exfoliated structure is concerned, no more diffraction peaks are apparent in the XRD patterns. This may be either the result of a space increase between the layers or a consequence of a non-ordered structure formation. Upon addition of MMT to the polymer matrix, the reflection peak disappeared, revealing a disordered and undetectable XRD owing to a homogeneously dispersed structure formation. In addition, Figure 2 shows that the nanocomposite structure is not affected by the presence of LEO. These results are in good agreement with those obtained by Abdollahi et al. [27] and by Alboofetileh et al. [28].

Optical microscopy

Optical microscopic images illustrating the dispersion of LEO in the matrix are shown in Figure 3. While

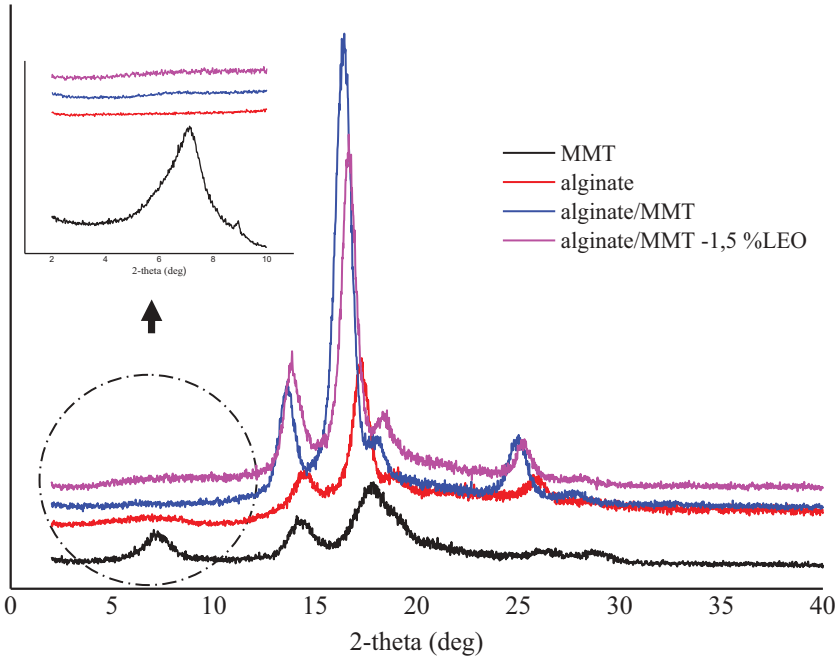

Figure 2. X-ray diffraction of MMT and sodium alginate-based nanocomposite films.

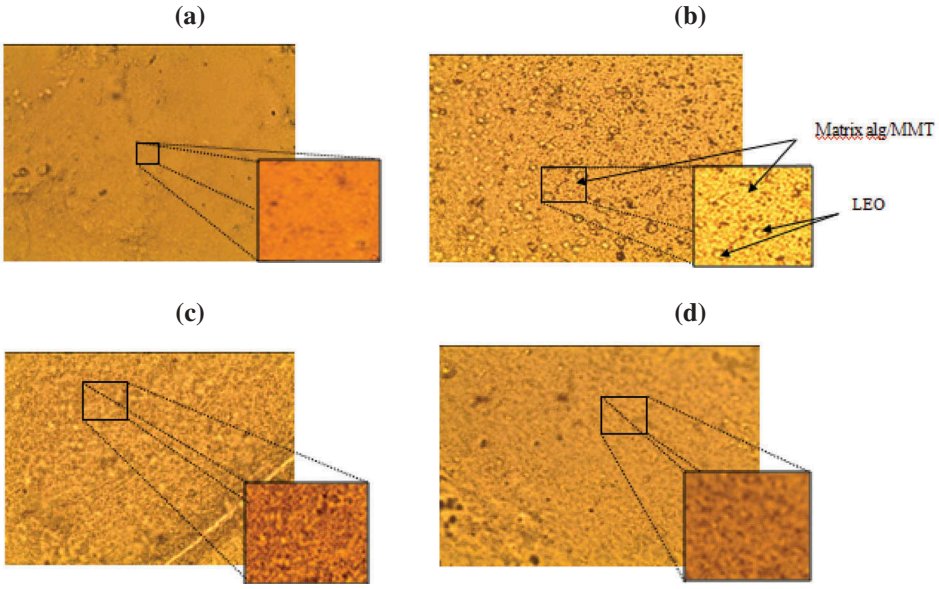

Figure 3. Morphology of (a) alginate/MMT, (b) alginate/MMT/LEO 0,5%, (c) alginate/MMT/LEO 1%, and (d) alginate/MMT-LEO1,5%.

a smooth and continuous structure is observed in LEO-free alginate/MMT film, fundamentally different aspects are visible in LEO-added materials. Surface discontinuities associated with the presence of essential oil are likely pointing to the formation of two phases in the matrix. At increasing LEO concentrations (0.5%, 1% and 1,5%), a random dispersion of LEO in alginate/MMT composites is observed with no significant essential oil phase-agglomeration. This observation is pertained to the fairly good miscibility between the LEO and the matrix which might be due to the creation of LEO's smaller and uniform micro-domains within the matrix, or otherwise stated to a nanoscale LEO distribution.

FTIR analysis

FT-IR analysis of the composite material structure unravels some interesting features closely linked to the complex nature of interactions existing between the material's components.

The characteristic bands of montmorillonite indicate SiOH hydroxyl stretching at 3619 cm^{-1} and H_2O hydroxyl bending at 1632 cm^{-1}. Bands centred at 993

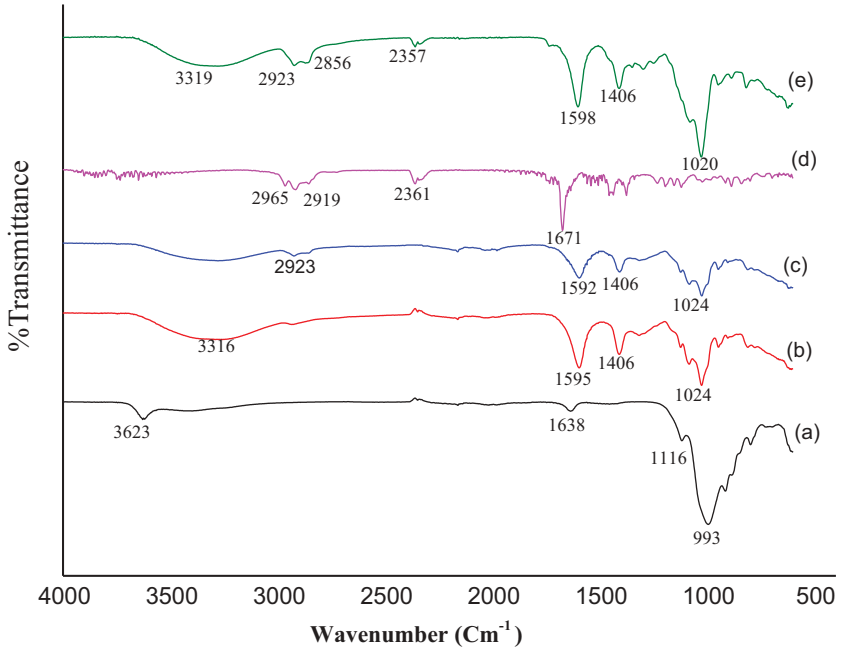

Figure 4. FTIR spectra of (a) MMT, (b) alginate, (c) alg/MMT, (d) LEO and (e) alg/MMT-LEO 1.5% films.

and 1116 cm^{-1} are attributed to the stretching vibration of the Si–O bonds [29,30] and Si–O–Si stretching (in-plane) vibration for silicates, respectively (Figure 4(a)). As shown in Figure 4(b), sodium alginate presents asymmetric and symmetric carboxylate stretching vibrations at 1595 and 1406 cm^{-1} and an oxygen stretching band at 1025 cm^{-1} for cyclic ether bridge. The band at 3317 cm^{-1} corresponds to OH stretching vibration [31]. Upon mixing alginate with MMT, the FTIR spectrum of the alg/MMT composite shows the combination of characteristic absorptions and the newly formed interactions between sodium alginate and montmorillonite groups (Figure 4(c)). For instance, disappearance of the 3619 cm^{-1} band assigned to silanol group of MMT surface in the nanocomposite spectrum may be explained by the hydrogen bonding between the silanol hydroxyl groups and alginate carboxyl and hydroxyl groups [32]. The other bands observed, and showing the incorporation of montmorillonite within alginate, are the COO^{-} (1595 and 1406 cm^{-1}) alginate stretching bands that has shifted to 1591 and 1409 cm^{-1}, respectively, in the composite. This shift comes from the developing interactions between – OH and carboxyl groups in the alginate surface. Thus, the FTIR spectrum of the alg/MMT confirms the interaction between alginate and montmorillonite. Furthermore, analysis of Figure 4(e) shows that the major bands present in the spectra of alg/MMT are also prominent in the oil-loaded nanocomposites, revealing a strong interaction between alginate and montmorillonite in the nanocomposites even after essential oil addition. However, some new bands are formed due to the presence of essential oil. The shift indicates a highly possible and successful interaction of oil with the nanocomposite. Major peaks at 3319, 2926 and 1601 cm^{-1} in lemon oil-loaded nanocomposite indicate the presence of C-H, O-H and C = O functional groups, respectively.

Thermal properties

The determination of films thermal behaviour intended to packaging commodities is critical from the standpoint of temperature interval of use. Indeed, inasmuch exposure of packaging films to extreme temperature variations such as heating, freezing or microwave irradiation is common [33], important structural changes of polymer films may befall. Thermogravimetric analyses of the neat alginate matrix and nanocomposites of alg-MMT and alg-MMT-LEO (1,5%) were undertaken. The thermograms illustrated (ATG-DTA) in Figure 5 show a common trend in terms of weight loss for all the

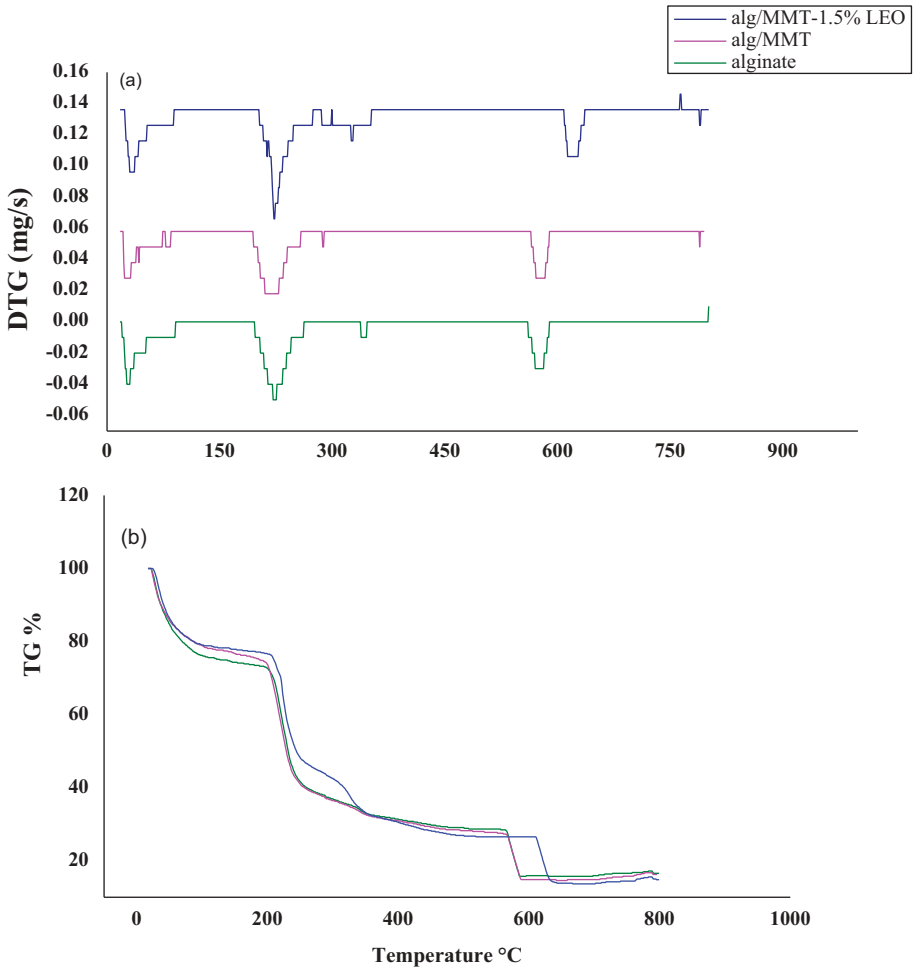

Figure 5. Thermogram DTG (a) et ATG (b) for alginate-based nanocomposite.

Table 1. Material weight loss (Δm) determined using thermal analysis data.

	Température °C					
Material	20–150	150–300	300–630	630–700	700–800	Δm (%) 20–800
Alginate	25.75	37.34	7.91	13.12	0.6	85
Alg-MMT	22.91	40.35	8.37	13.52	1.45	84.7
Alg-MMT -1.5%LEO	22.23	35.65	15.32	13.01	1.05	84.6

Table 2. Thickness and opacity values of Alg/MMT nanocomposite films.

Film	Thickness (mm)	Opacity
Alginate	0.0225 ± 0.006	2.04 ± 0.003
Alg/MMT	0.0260 ± 0.018	2.33 ± 0.044
Alg/MMT-LEO 0.5%	0.0250 ± 0.002	9.808 ± 0.00
Alg/MMT-LEO1%	0.032 ± 0.006	11.35 ± 0.227
Alg/MMT-LEO1.5%	0.0330 ± 0.026	10.31 ± 0.40

samples whose degradation occurs in 03 distinct and similar stages. Data of weight-loss at different temperatures are summarised in Table 1.

The first weight loss occurred between 20°C and 150°C for all samples. 25.75, 23 and 22% weight loss values of alginate film, alg-MMT and alg-MMT -LEO, respectively, were observed. The initial weight loss originates from the release of moisture and relatively high water contents that are present in alginate and alg/MMT nanocomposite films. A second weight loss monitored between 150°C and 300°C for all samples is presumably resulting from structure degradation of alginate film located inside MMT interlayer space. An additional weight loss recorded for alg-MMT/LEO films between 300°C and 630°C (15.32%) is reasonably ascribed to LEO loaded into the film matrix. In general, the second and third stage's degradation temperature of alg-MMT/LEO film was higher than the other films. A similar thermal behaviour has been reported in the literature in which EO was added to cellulose acetate/MMT composite material [34]. The greater thermal stability of LEO-containing alginate samples seems resulting from interaction between alginate and LEO, yielding a thermally resistant polymer matrix. Above 630°C, all curves are consistent since the remaining substances were mainly inorganic residues.

Film thickness and opacity values of Alg/MMT nanocomposite films

Thick and opaque films were obtained upon addition of oil whereas pure alginate film was thin and transparent. Variations in film thickness influence mechanical and barrier properties, and thus thickness uniformity is a quality-tied processing parameter. Table 2 summarises films thickness. The average thickness was less than 100 micrometres delivering flexible film. Upon addition of increasing amount of LEO, films became thicker. As a plausible explanation, we think that low molecular weight LEO components fit into alginate polymer chains and expand the polymeric network. Such plasticising effect, similarly described in the literature, is probably a major factor leading to observed growing film thickness [35].

Opacity is an established optical measurement of film transparency, and so it constitutes a relevant property since it has a direct impact on the appearance of the packaged product. Presence of essential oil in the nanocomposite films modifies their optical appearance and light barrier properties. Opacity of

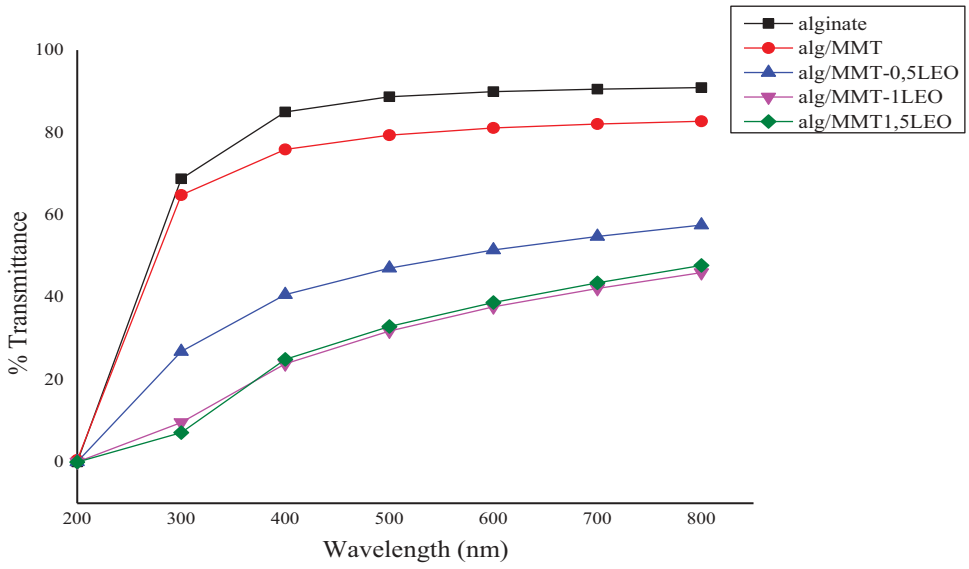

Figure 6. Transmittance versus wavelength relationship for alginate and nanocomposite films.

nanocomposite films is reported in Table 2. The opacity value of alginate film taken as reference was 2.04 ± 0.003, whereas, upon addition of LEO at increasing concentrations opacity changed proportionally to 11.35 ± 0.227. Hence, EO's-free films were more transparent than their EO-containing counterparts. UV-visible light transmission of the nanocomposite films containing various concentrations of LEO in the 200–800 nm wavelength interval is shown in Figure 6. Clearly, EO-containing films are able to stop ultraviolet radiation in the region of 280 nm. Decreased light transmission is likely due to light scattering at the surface of essential oil droplets in the film matrix [36]. Hence, this phenomenon is able to postpone oil oxidation and prevent nutrient losses, discolouration, and off-flavours in food systems. Our results are consistent with similar findings that have been reported in the literature. Ahmad et al. [37] and by Atef et al. [38].

Antibiogram test and antimicrobial effectiveness of films

The antimicrobial activity of LEO-containing nanocomposite films of various concentrations (0.5%, 1% and 1.5%) deposited on filter paper discs against selected microorganisms is shown in Table 3. LEO-free alg/MMT nanocomposite film, which served as control, did not show any antibacterial effect as witnessed by the absence of inhibition zones. The highest antibacterial activity was recorded for alg-MMT films containing 1.5% LEO (Figure 7). Noteworthy, among the bacterial strains that were tested, *E. coli* and *S. enteritidis* proved more resistant to active films because they are Gram-negative bacteria and as such, they are prone to higher resistance towards antimicrobial compounds owing to their extra protective outer membrane [39]. In this regard, the essential oil showed its best antibacterial activity in the disc diffusion test on Gram-positive bacteria (i.e. *B.cereus, S.aureus*). Consequently, the antimicrobial efficacy of LEO-containing films is clearly due to the presence of LEO, which contains a plethora of terpene derivatives whose presence is strongly connected to antimicrobial action. Indeed, it has been reported that monoterpene or sesquiterpene hydrocarbons and their oxygenised derivatives, which are the major components of essential oils, exhibit potential antimicrobial activities [40]. Seemingly, these compounds are able to disintegrate the cytoplasmic membrane of bacteria and thereby triggering a series of events such as disrupting the proton motive force, electron flow, active transport, and/or coagulation of cell contents [41].

Table 3. Antibacterial activity (inhibitory zone) of alg-MMT solution films incorporated with LEO against gram-positive and gram-negative bacteria.

Bacterial strain	con(v/v)% in Solution films	Inhibition diameter
Staphylococcus aureus (Gram+)	Control	R
	0.5	10.66 ± 0.57
	1	18.66 ± 0.57
	1.5	20.33 ± 1.52
Bacillus cereus (Gram+)	Control	R
	0.5	11.66 ± 1.15
	1	14.33 ± 057
	1.5	17 ± 1
Escherichia coli (Gram-)	Control	R
	0.5	10.5 ± 0.5
	1	10.66 ± 0.57
	1.5	11.6 ± 0.57
Salmonella enteritidis (Gram-)	Control	R
	0.5	9.33 ± 0.57
	1	11 ± 1
	1.5	10.66 ± 1.52

In addition to the inhibition zone tests, which provide qualitative assessment of the antibacterial properties of the films, quantitative antibacterial studies of alg MMT/LEO films were performed in accordance with TSA-3% NaCl in step model. The relationship between *S.aureus and E.coli*'s growth, taken as models of Gram+ and Gram- bacteria, respectively, and LEO-contatining alginate films is presented in Figure 8.

Figure 8(a) shows curves of *S.aureus* growth in TSA-3% NaCl loaded with alginate base films. For comparison purpose, TSA-3% NaCl containing solely *S.aureus* was taken as reference during the same storage period. The initial *S.aureus* population in the reference plate was 2 log CFU/cm^2. The microbial counting increased substantially during the storage attaining 7.48 log CFU/cm^2. Our results are in good agreement with data recently reported in the literature [42]. Furthermore, low antimicrobial activity was observed in plates coated with alginate/MMT film during the storage period. The lowest *S.*

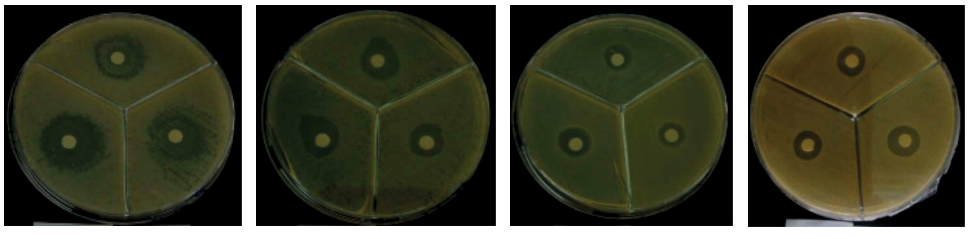

Figure 7. Antibacterial effect of alg-MMT solution films: (a) *Staphylococcus aureus*; (b) *Bacillus cereus*; (c) *Escherichia coli*; (d) *Salmonella enteritidis* at 1.5% concentration of LEO.

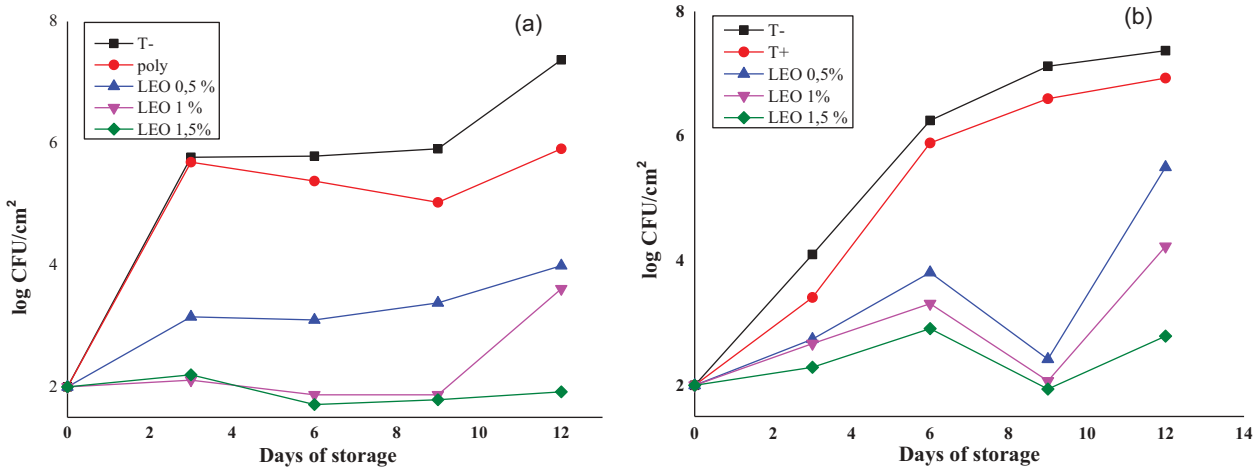

Figure 8. Antibacterial activity of different films against (a) *S .aureus* and (b) *E.coli* on TSA- NaCl (3%) medium stored at 10°C.

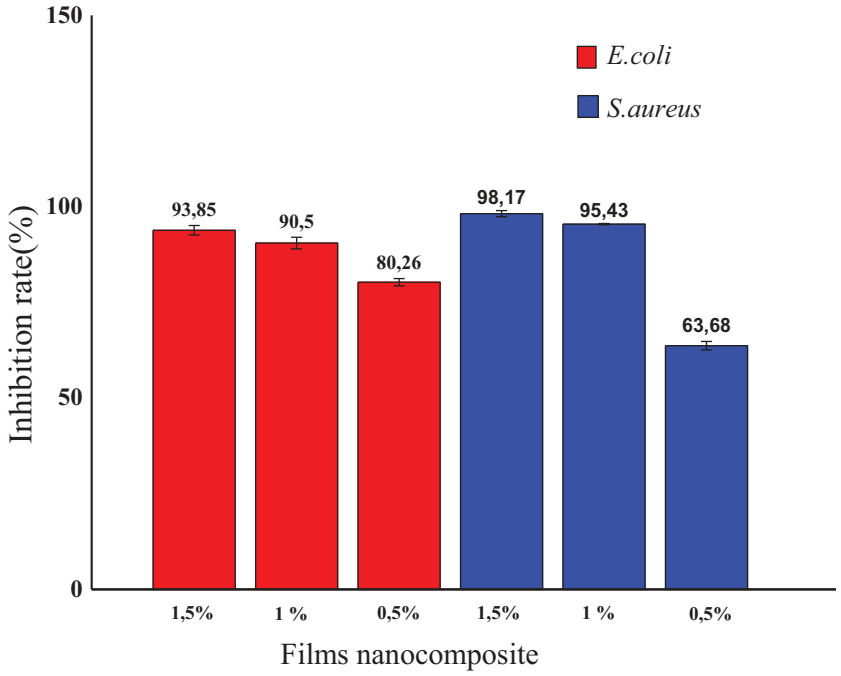

Figure 9. Inhibition tests.

aureus population was found for LEO-containing films at 1.5% LEO concentration, by maintaining the population below the initial inoculation level (1.92 log CFU/cm^2). At lower LEO concentration (1%), the film matrix showed less antimicrobial activity as total inhibition of microorganism growth was noted during the first 6 days of the storage period. After 12 days, films containing 1% LEO reduced the growth to 3.61 log CFU/cm^2, as compared with the control assay. As expected, at lower LEO contents (0,5%) the films proved less efficient in terms of antimacrobial activity.

Figure 8(b) shows *E.coli's* growth in the TSA-3% NaCl reference test and in TSA-3% NaCl plates comprising LEO-containing films at different concentrations. The microbial count increased in the reference plate from 2 log CFU/cm^2 to 7.3 log CFU/cm^2 by the end of the experiment (12 days). At LEO concentration of 1.5%, a total inhibition was observed during the first 6 days of experiment, with a counted population of 2.29 CFU/cm^2. At 1% LEO contents, a complete inhibition of microbial growth was observed during the 6 days of storage and reduced to

Table 4. Antifungal activity (inhibitory zone) of alg-MMT solution films incorporated with LEO against *Candida albicans* and *Aspergillus braziliensis.*

Fungal strain	con(v/v)in solution films %	Inhibition diameter
Candida albicans	Control	R
	0.5	9.33 ± 0.57
	1	10 ± 1
	1.5	10.66 ± 0.57
Aspergillus brasiliensis	Control	R
	0.5	23 ± 1.52
	1	23.33 ± .1.52
	1.5	30 ± 1

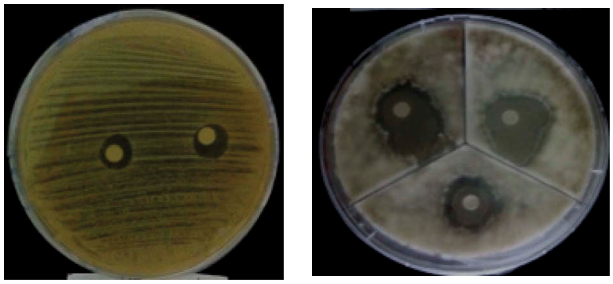

-e- -f-

Figure 10. Antifungal effect of alg-MMT solution films; (e) *Candida albicans*; (f) *Aspergillus brasiliensis* at 1.5% concentration of LEO.

2.67 CFU/cm^2. However, low antimicrobial action was observed for films containing 0.5% LEO.

Figure 9 illustrates the trend of nanocomposite films inhibition effect in terms of LEO's concentration variations (0.5%, 1% and 1.5%). The most concentrated LEO sample (1,5%) exhibited the highest inhibition rate with 93,8% and 98,2% of *E. coli* and *S. aureus* growth inhibition after 12 days, respectively.

Antifungal activity measurement

Antifungal experiments were carried out with *Candida albicans* and *Aspergillus brasiliensis*.

Candida albicans is an opportunistic fungal pathogen that exists as a harmless commensal in the gastrointestinal and genitourinary tracts of 70% of humans and about 75% of women suffer from *Candida* infection at least once in their lifetime [43–46]. However, it becomes an opportunistic pathogen for immunocompromised patients as well as some immunologically weak individuals, or even for healthy persons.

The fungus *Aspergillus brasiliensis*, the most important species of Aspergillus genus, is a type of mould that is nearly ubiquitous in our environment. Although *A. brasiliensis* is also an industrially important fermentation strain, producing many enzymes, such as amylase, cellulase, and pectinase [47], it constantly causes food spoilage, industrial and agricultural products mouldy, and mycotoxin pollution (ochratoxin A). Especially, *A. brasiliensis* might induce otomycosis and pulmonary infections in immunocompromised persons [47].

Table 4 summarises the results of the in vitro studies conducted with *C.albicans* and *A. brasiliensis*. The alg-MMT/LEO had an antifungal effect on the two fungi; however, the antifungal effect was more potent on *Aspergillus barasiliensis* than on *C.albicans* (Figure 10). Fungi susceptibility showed that alg-MMT/LEO film produced a 30 mm in diameter inhibition zone against *Aspergillus brasiliensis* thus presenting a high antifungal activity.

Conclusion

In this study, the biocidal efficiency of alg-MMT /LEO films against two fungal and four bacterial strains was addressed. The antimicrobial films were easily prepared by controlled addition of LEO into alginate/MMT films at different concentrations. The results revealed that LEO-containing films were more effective against Gram-positive bacteria (*S. aureus* and *B. cereus*) than Gram-negative bacteria (*E. coli* and *S.enteritidis*). Furthermore, a complete growth inhibition was observed for the films containing the highest concentration of lemon essential oil (i.e. 1,5%) in each of the four bacteria. As a preliminary foray in antifungal activity perspectives, evidence that alg-MMT/LEO films exhibit excellent antifungal activity against *A. brasiliensis*, used as model pathogenic fungus was provided. Thus, owing to their broad-spectrum antimicrobial efficacy, the potential for antimicrobial food packaging applications of these new films has clearly been demonstrated and will hopefully contribute to the advance of ecofriendly food packaging plastics.

Disclosure statement

No potential conflict of interest was reported by the authors.

References

[1] Rhim J, Ng P. Natural biopolymer-based nanocomposite films for packaging applications. Crit Rev Food Sci Nutr. 2007;47(4):411–433. doi:10.1080/10408390600846366

[2] Wong D, Camirand W, Pavlath A. 1994.Development of edible coatings for minimally processed fruits and vegetables. In: Krochta JM, Baldwin EA, Nisperos-Carriedo MO, editors. Edible coatings and films to improve food quality. Lancaster, PA: Technomic Publishing Co. pp. 65–88.

[3] Liang B, Zhao H, Zhang Q, et al. Ca^{2+} enhanced nacre-inspired montmorillonite–alginate film with superior mechanical, transparent, fire retardancy, and shape memory properties. ACS Appl Mater Interfaces. 2016;8(42):28816–28823.

[4] Alboofetileh M, Rezaei M, Hosseini H, et al. Morphological, physico-mechanical, and antimicrobial properties of sodium alginate-montmorillonite nanocomposite films incorporated with marjoram essential oil. Crit Rev Food Sci Nutr. DOI:10.1111/jfpp.1359
[5] Tezcan F, Günister E, Ozen G, et al. Biocomposite films based on alginate and organically modified clay. Int J Biol Macromol. 2012 May 1;50(4):1165–1168. . Epub 2012 Jan 14.
[6] Barreca S, Orecchio S, Pace A. The effect of montmorillonite clay in alginate gel beads for polychlorinated biphenyl adsorption: isothermal and kinetic studies. Appl Clay Sci. 2014;99:220–228.
[7] Zlopasa J, Norder B, Koenders EAB, et al. Origin of highly ordered sodium alginate/montmorillonite bionanocomposites. Macromolecules. 2015;48 (4):1204–1209.
[8] Cerisuelo JP, Bermudez JM, Aucejo S, et al. Describing and modeling the release of an antimicrobial agent from an active PP/EVOH/PP package for salmon. Food Eng. 2013; 116–352.
[9] Silvestre C, Duraccio D, Cimmino S. Food packaging based on polymer nanomaterials. Prog Polym Sci. 2011;36:1766.
[10] Bradley EL, Castle L, Chaudhry Q. Applications of nanomaterials in food packaging with a consideration of opportunities for developing countries. Trends Food Sci Tech. 2011;22:604.
[11] Manjula B, Babul RA, Varaprasad K, et al. Silver nanoparticles incorporated within intercalated clay/polymer nanocomposite hydrogels for antibacterial studies. Polym Compos. 2016;36:2220.
[12] Yongjian X, Leigang Z, Tao L, et al. Preparation and characterization of cellulose/Ag nanocomposites. Polym Compos. 2014;36:2220.
[13] Ramos-Corella KJ, Sotelo-Lerma M, Gil-Salido AA, et al. Controlling crystalline phase of TiO2 thin films to evaluate its biocompatibility. Mater Technol. 2019;34:455–462.
[14] Liu H, Li DR, Yang XL, et al. Fabrication and characterization of Ag3PO4/TiO2 heterostructure with improved visible-light photocatalytic activity for the degradation of methylorange and sterilization of E. coli. Mater Technol. 2019;34:192–203.
[15] Depan D, Misra RDK. On the determining role of network structure titania in silicone against bacterial colonization: mechanism and disruption of biofilm. Mater Sci Eng C Mater Biol Appl. 2014 Jan 1;34:221–228.
[16] Girase B, Depan D, Shah JS, et al. Silver-clay nanohybrid structure for effective and diffusion-controlled antimicrobial activity. Mat Sci Eng C-Mater. 2011;31:1759–1766.
[17] Devesh R, Misra RDK, Girase B, et al. Hybrid nanoscale architecture for enhancement of antimicrobial activity: immobilization of silver nanoparticles on thiol-functionalized polymer crystallized on carbon nanotubes. Adv Biomater. 2012;14:B 93–100.
[18] Venkatasubramanian R, Srivastava RS, Misra RDk. A comparative study of antimicrobial and photocatalytic activity of different dopants in titania-encapsulated nanoparticle composites. Adv Mater Res Switz. 2008;24,:589–595.
[19] Hosseini SF, Rezaei M, Zandi M, et al. Bio-based composite edible films containing Origanum vulgare L. essential oil. Ind Crops Prod. 2015;67:403.
[20] Kennedy LB, Peng JF, Yie JLX, et al. Preparation and performance evaluation of glucomannan-chitosan-nisin ternary antimicrobial blend film. Carbohydr Polym. 2006;65:488–494.
[21] Cha DS, Cooksey DK, Chinnan MS, et al. Release of nisin from various heat-pressed and cast films. LWT - Food Sci Technol. 2003;36:209–213.
[22] Cagri A, Ustunol Z, Ryser ET. Antimicrobial edible films and coatings. J Food Prot. 2004;67:833–848.
[23] Rico-Pena DC, Torres JA. Sorbic acid and potassium sorbate permeability of an edible film methylcellulose-palmitic acid film: water activity and pH effects. J Food Sci. 1991;56:1991–1995.
[24] Kim YD, Morr CV. Microencapsulation properties of gum arabic and several food proteins: spray-dried orange oil emulsion particles. J Agr Food Chem. 1996;44:1314–1320.
[25] Rodrigues GH, Susin I, Pires AV, et al. Replacement of corn by citrus pulp in high grain diets fed to feedlot lambs. Ciência Rural, Santa Maria. 2008;38 (3):789–794.
[26] Donsi F, Annunziata M, Sessa M, et al. Nanoencapsulation of essential oils to enhance their antimicrobial activity in foods. LWT - Food Sci Technol. 2011;44:1908–1914.
[27] Abdollahi M, Rezaei M, Farzi G. .A novel active bionanocomposite film incorporating rosemary essential oil and nanoclay into chitosan. J Food Eng. 2012;111:343–350.
[28] Alboofetileh M, Rezaei M, Hosseini H, et al. Efficacy of activated alginate-based nanocomposite films to control Listeria monocytogenes and spoilage flora in rainbow trout slice. J Food Sci Technol. 2016 January;53:521–530.
[29] Zhou CH, Zhang D, Tong DS, et al. Paper-like composites of cellulose acetate–organo-montmorillonite for removal of hazardous anionic dye in water. Chem Eng J. 2012;209:223.
[30] Kumar SK, Ramachandran R, Kalidhasan S, et al. Potential application of dodecylamine modified sodium montmorillonite as an effective adsorbent for hexavalent chromium. Chem Eng J. 2012;211/212:396.
[31] Iliescu RI, Andronescu E, Ghitulica CD, et al. Montmorillonite–alginate nanocomposite as a drug delivery system – incorporation and in vitro release of irinotecan. Int J Pharm. 2014;463:184.
[32] Giovanni S, Franca B, Andrea P, et al. Electrophilic alkenylation of aromatics with phenylacetylne over zeolite HSZ-360. Tetrahedron Lett. 1995;36:9177–9180.
[33] Hsieh TH, Ho KS. Effects of thermal stability on the crystallization behavior of poly(vinylidene chloride). J Polym Sci. 1999;37:3269–3276.
[34] Polaa CC, Medeirosa EAA, Pereirab OLL, et al. Cellulose acetate active films incorporated with oregano (Origanum vulgare) essential oil and organophilic montmorillonite clay control the growth of phytopathogenic fungi. Food Pack Shelf Life. 2016;9:69–78.
[35] Krkić N, Lazić V, Gvozdenović J. Chitosan biofilm properties as affected by the addition of oregano essential oil. J process energy griculturea. 2013;15 (3):165–168.
[36] Tongnuanchan P, Benjakul S, Prodpran T. Properties and antioxidant activity of fish skin gelatin film

incorporated with citrus essential oils. Food Chem. 2012;134:1571–1579.
[37] Ahmad M, Benjakul S, Prodpran T, et al. Physico-mechanical and antimicrobial properties of gelatin film from the skin of unicorn leatherjacket incorporated with essential oils. Food Hydrocoll. 2012;28:189–199.
[38] Atef M, Rezaei M, Behrooz R. Characterization of physical, mechanical, and antibacterial properties of agar-cellulose bionanocomposite films incorporated with savory essential oil. Food Hydrocoll. 2015;45:150–157.
[39] Cozmuta AM, Turilaa A, Apjoka R, et al. Preparation and characterization of improved gelatin films incorporating hemp and sage oils. Food Hydrocoll. 2015;49:144–155.
[40] Cakir A, Kordali S, Zengin H, et al. Composition and antifungalactivity of essential oils isolated from hypericum hyssopifolium and hypericum heterophyllum. Flav Frag J. 2004;19:62.
[41] Burt S. Essential oils: their antibacterial properties and potential applications in foods-a review. Int J Food Microbiol. 2004;94(3):223–253.
[42] Rezaei M, Alboofetileh M, Hosseini H, et al. Morphological, physico-mechanical, and antimicrobial properties of sodium alginate-montmorillonite nanocomposite films incorporated with marjoram essential oil. J Food Process Preserv. 2018;42(5):e 13596.
[43] Ruhnke M, Maschmeyer G. Management of mycoses in patients with hematologic disease and cancer—review of the literature. Eur J Med Res. 2002;7(5):227–235.
[44] Meiller TF, Hube B, Schild L, et al. A novel immune evasion strategy of *Candida albicans*: proteolytic cleavage of a salivary antimicrobial peptide. PLoS One. 2009;4(4):e5039.
[45] Schulze J, Sonnenborn U. Yeast in the gut: from commensals to infectious agents. Deutsches Arzteblatt. 2009;106(51–52):837–842.
[46] Sobel JD. Vaginitis. N Engl J Med. 1997;337(26):1896–1903.
[47] Tolouee M, Alinezhad S, Saberi R, et al. Effect of matricaria chamomilla L. flower essential oil on the growth and ultrastructure of Aspergillus niger van Tieghem. Int J Food Microbiol. 2010;139:127–133.